# Kinetic Properties of GABA $\rho$1 Homomeric Receptors Expressed in HEK293 Cells

Jay Yang, Qing Cheng, Ayako Takahashi, and Farida Goubaeva
Department of Anesthesiology, Columbia University College of Physicians & Surgeons, New York, New York 10032

ABSTRACT The $\rho$1 subunit of the ionotropic GABA receptors is thought to contribute to the formation of the $GABA_C$ receptors with pharmacological and physiological properties distinct from those of $GABA_A$ receptors. Previous characterization of this subunit expressed in the *Xenopus* oocytes revealed an ion channel with slow activation and deactivation and no desensitization, quite different from the properties of $GABA_C$ receptors observed in native cells. We expressed the human $\rho$1 subunit in human embryonic kidney (HEK) 293 cells and quantitatively characterized the kinetic properties of these receptors using a rapid drug application device. The $\rho$1 subunit expressed in HEK293 cells exhibited pharmacological and kinetic properties qualitatively identical to those described when $\rho$1 was expressed in the oocytes. An apparent desensitizing current observed during a constant GABA application was determined to be secondary to an $E_{Cl}$ shift. Detailed kinetic analyses and parameter estimation for a five-state kinetic model revealed that the channel is best described by a set of rate constants with a notably faster GABA unbinding $K_{off}$ rate compared to the parameters proposed for the same subunit expressed in the oocytes. The same subunit expressed in hippocampal neurons showed activation and deactivation kinetics identical to the current characterized in HEK293 cells. The kinetic properties of $\rho$1 subunit expressed in a nonoocyte model system may be better described quantitatively by the rate constants presented here.

## INTRODUCTION

The human $\rho$1 subunit of the ionotropic GABA receptors forms functional ion channels with properties distinct from the $GABA_A$ receptors when expressed in *Xenopus* oocytes. The homomeric $\rho$1 receptors exhibit insensitivity to bicuculline, barbiturate, or benzodiazepine with essentially no desensitization in the continued presence of GABA (1). Quantitative characterization revealed the $\rho$1 homomeric receptors to be 40 times more sensitive to GABA, to activate 8.3-fold more slowly, and to close eightfold more slowly than a prototypic $\alpha\beta\gamma$ $GABA_A$ receptor (2). A careful concentration-response study using a combination of wild-type and activation-impaired mutant $\rho$1 led to a kinetic activation model in which GABA occupation of three of the five identical GABA-binding sites leads to the channel opening (3). Further parameter estimation using a concurrent direct [$^3$H]GABA binding and voltage-clamp study identified an optimum kinetic model most notable for the slow association constant, where the ligand binding rate is three orders of magnitude slower than diffusion and the trapping of the ligand by the opened receptor slowing the ligand dissociation (4).

More recently, the human $\rho$1 subunit has been expressed in mammalian cells including human embryonic kidney (HEK) 293 cells and rat hippocampal neurons (5–7). In general, the GABA-evoked currents mediated by the homomeric $\rho$1 receptors expressed in HEK293 cells demonstrated relative permeability to anions (8), resistance to bicuculline, and slow deactivation rate (5) qualitatively similar to the properties of these channels well characterized in the *Xenopus* oocyte expression system. However, the quantitative details of the $\rho$1 homomeric channels expressed in the HEK293 cells differ considerably from the same subunits expressed in the *Xenopus* oocytes, particularly with respect to the deactivation kinetics and the apparent desensitizing response in the continued presence of GABA.

A quantitative understanding of the $\rho$1 homomeric channel behavior in a mammalian expression system is a prerequisite in understanding how these receptors may work in mammals. We used a piezoelectric driver-based rapid solution exchange system to quantitatively characterize the kinetics of homomeric $\rho$1 receptors expressed in HEK293 cells and interpreted the resulting data in the context of the five-state model proposed by Weiss.

## MATERIALS AND METHODS

### Cell culture

HEK293 cells (ATCC, Manassas, VA) seeded at a density of $5 \times 10^5$ cells/35-mm dish maintained in DMEM supplemented with 10% fetal bovine serum and antibiotics were transiently transfected with the indicated plasmids using Lipofectamine Plus (Invitrogen, Carlsbad, CA) following the manufacturer's recommended protocol. The human $\rho$1 cDNA kindly provided by Dr. Cutting (Johns Hopkins University) was subcloned into the pCI/neo (Promega, Madison, WI) eukaryotic expression plasmid and 1.5 $\mu$g $\rho$1-pCI/neo + 0.5 $\mu$g pEGFP (Invitrogen) per dish used for transfection. The transfected cells identified under an epifluorescent microscope were used for patch-clamp experiments 24–48 h after transfection.

*Submitted March 21, 2006, and accepted for publication June 9, 2006.*

Address reprint requests to Jay Yang, MD, PhD, Dept. of Anesthesiology, Columbia University College of Physicians & Surgeons, 630 West 168th St., PH5, New York, NY 10032. Tel.: 212-342-0023; Fax: 212-305-0777; E-mail: jy2029@columbia.edu.

Qing Cheng's present address is Dept. of Neurobiology, Duke University School of Medicine, Durham, NC 27708.



0006-3495/06/09/2155/08 $2.00

doi: 10.1529/biophysj.106.085431

Neonatal (from 1 to 2 days old) Sprague Dawley rat pups deeply anesthetized with halothane were decapitated, and the hippocampi dissected out in ice-cold $Ca^{2+}$- and $Mg^{2+}$-free Hanks' balanced salt solution. The tissue was enzymatically digested with papain and bovine serum albumin (1 mg/ml for each) (Sigma, St. Louis, MO) for 20 min at 37°C. Cells were disaggregated by trituration and plated on Matrigel-coated 35-mm tissue culture plates (Becton Dickinson, Bedford, MA) in Neurobasal medium (Invitrogen) supplemented with 2 mM L-glutamine, 10% fetal calf serum (Hyclone, Logan, UT), 5% horse serum, and B-27 supplement (Invitrogen). After 2–3 days of growth in a 95% $O_2$/5% $CO_2$ humidified incubator at 37°C, the dishes were treated with 10 $\mu$M cytosine arabinoside for 24 h to suppress the growth of glial cells. Thereafter, the medium was switched to a Neurobasal containing 5% horse serum and changed every 2–4 days until used for experiments. The hippocampal culture was transduced with an approximate multiplicity-of-infection (MOI) of 10 with adenovirus designed to express both the $\rho$1 subunit and the reporter EGFP protein (see Cheng et al. (7) for details). The transduced hippocampal neurons were visually identified for the patch-clamp experiment.

## Electrophysiology

Patch electrodes were pulled from 1.5-mm OD borosilicate capillary glass (WPI, Sarasota, FL) and fire polished. Typical electrodes had a resistance of 5–10 M$\Omega$ when filled with intracellular solutions. The intracellular solution consisted of (in mM): 140 CsCl, 4 NaCl, 2 $MgCl_2$, 10 K-EGTA, 10 HEPES, titrated to pH 7.3 with CsOH, and supplemented with 2 mM Mg-ATP. The external solution contained (in mM): 140 NaCl, 2.8 KCl, 1 $MgCl_2$, 3 $CaCl_2$ 10 HEPES, 10 glucose, and was titrated to pH 7.4 with NaOH. For hippocampal neurons, TTX 1 $\mu$M was added to the external solution to inhibit action potentials. Recordings were made using an AxoPatch 200A amplifier (Axon Instruments, Foster City, CA). A typical access resistance of ~15 M$\Omega$ in the whole-cell mode of patch clamp was limited to 75% electronic compensation without causing instability. Voltage measurement errors resulting from uncompensated series resistance for large currents underreport the true current, possibly underestimating the degree of apparent desensitization. The cell input capacitance was approximated by directly reading off the capacitance compensation dial of the amplifier. Recorded membrane currents were filtered at 5 kHz, digitized using Clampex v8.0, and analyzed with Clampfit v6.0 (Axon Instruments). A syringe pump delivered the external solution at 15 ml/h through orifices of a $\theta$ tube mounted on a piezoelectric transducer (Burleigh Instruments, Fishers, NY). This perfusion rate was determined after a series of careful preliminary experiments looking at the time course of shift in the whole-cell holding current in response to application of a high-potassium (100 mM $K^+$) solution. Command steps at 120-s intervals rapidly moved the perfusion ports, exposing the cell to either the control or the drug solution. At this GABA application interval, no decrease in the peak response to 100 $\mu$M GABA was noted. The perfusion device allowed exchange of solution in ~15 ms (10–90% rise time) for the whole-cell recording configuration. All experiments were performed at room temperature (20–25°C). Aqueous solutions of GABA and bicuculline methiodide, and DMSO solutions of etomidate and I4AA prepared as ×1000 stock were stored as frozen aliquots at −20°C and freshly diluted on the day of the experiments. The I4AA-blockable, bicuculline-resistant current seen in virally transduced hippocampal neurons has been thoroughly characterized and determined to be a $\rho$1 receptor-mediated current (7). Drugs were purchased from Sigma Chemicals.

## Model simulation

Simulations of the gating model were performed using the Q-matrix method written in Matlab (Mathworks, Natick, MA). A Q-matrix corresponding to the five-state gating model (see Fig. 4 *A*) was entered, and the time course of the state vector solved according to the matrix equation $\mathbf{X}(t) = e^{\mathbf{Q}(t)} * \mathbf{X}(0)$. $\mathbf{X}(t)$ is the 5 × 1 time-dependent state vector (i.e., $C_1$, $C_2$, $C_3$, $C_4$, O) at time $t$, $\mathbf{Q}(t)$ is the 5 × 5 Q-matrix, and $\mathbf{X}(0)$ is the 5 × 1 initial state vector equal to $[1\ 0\ 0\ 0\ 0]^T$. The simulation time was separated into two time epochs: during GABA application and on GABA removal. Within each of these epochs, the GABA concentration-dependent rates of the Q-matrix were held constant. Simulations during the two epochs correspond to the time course of activation/desensitization during GABA application and deactivation after GABA removal. The predicted rate constants and the respective coefficients describing the macroscopic activation and deactivation were calculated from the eigenvalues of the Q-matrix and a spectral matrix expansion of the Q-matrix as detailed in Colquhoun and Hawkes (9). The predicted steady-state response was taken as the sum of the row entry of the spectral matrix corresponding to the eigenvalue = 0. The model parameter optimization was accomplished by minimizing the sum squared error consisting of a linear sum of the errors from the concentration-response, the concentration-independent deactivation rate, and the limiting monoexponential activation rate at a high GABA concentration (i.e., $\alpha + \beta$). The concentration-response relationship was determined by fitting the equation: response = 1/(1 + (EC50/[GABA])^$n$) where EC50 is the concentration for half-maximal response and $n$ = Hill slope to the normalized empirical data or the maximum current attained during a 20-s GABA exposure for the simulated data. The final model parameters used for the simulation are shown in Table 1. The Matlab m-file codes implementing these routines are available from the corresponding author.

## RESULTS

Exogenous application of GABA to the voltage-clamped (−60 mV) HEK293 cells transfected with $\rho$1 subunit elicited an inward-going current (Fig. 1 *A*). The peak magnitude of the current depended on the GABA concentration as well described by a Hill equation with an EC50 = 2.11 $\mu$M and a slope = 2.08. The elicited current was notable for an apparent desensitization in the presence of higher GABA and a concentration-independent slow deactivation on removal of GABA (Fig. 1 *A*). The current was not blocked by

**TABLE 1 A comparison of optimized parameters for the five-state kinetic model shown in Fig. 4 *A***

| Model parameters | Oocyte | HEK Cell | Experimental |
|---|---|---|---|
| $\alpha$ ($s^{-1}$) | 0.31 | 0.16 | – |
| $\beta$ ($s^{-1}$) | 3.6 | 9.83 | – |
| $K_{on}$ ($\mu M^{-1}s^{-1}$) | 0.096 | 0.32 | – |
| $K_{off}$ ($s^{-1}$) | 0.18 | 4.59 | – |
| EC50 ($\mu$M) | 0.80 | 2.15 | 2.11 ± 0.15 |
| Slope | 2.37 | 2.09 | 2.08 ± 0.10 |
| $\tau_{deact}$ (s) at 1 $\mu$M | 26.4 | 10.7 | 11.0 ± 0.44 |
| $\tau_{act}$ (s) at 1 $\mu$M* | 5.83 | 6.46 | 5.9 ± 0.45 |
| 10–90% rise time (s) | 12.8 | 14.2 | 13.0 ± 2.30 |
| $\tau_{act}$ (s) at 30 $\mu$M* | 0.55 | 0.18 | 0.16 ± 0.01 |
| 10–90% rise time (s) | 1.2 | 0.4 | 0.38 ± 0.05 |

The parameters for the receptors expressed in oocytes system were taken from Chang and Weiss (4), but the calculations were done with our software implementation.

*The activation kinetics is clearly complex, demonstrating a sigmoidal activation as expected for a channel with multiple cascading states; therefore, the monoexponential fit listed is only an approximation of the true activation kinetics, which in theory is always a sum of four exponentials with time constants corresponding to the inverse of the nonzero eigenvalues of the Q-matrix. The 10–90% rise time was determined from the sum of four exponentials.

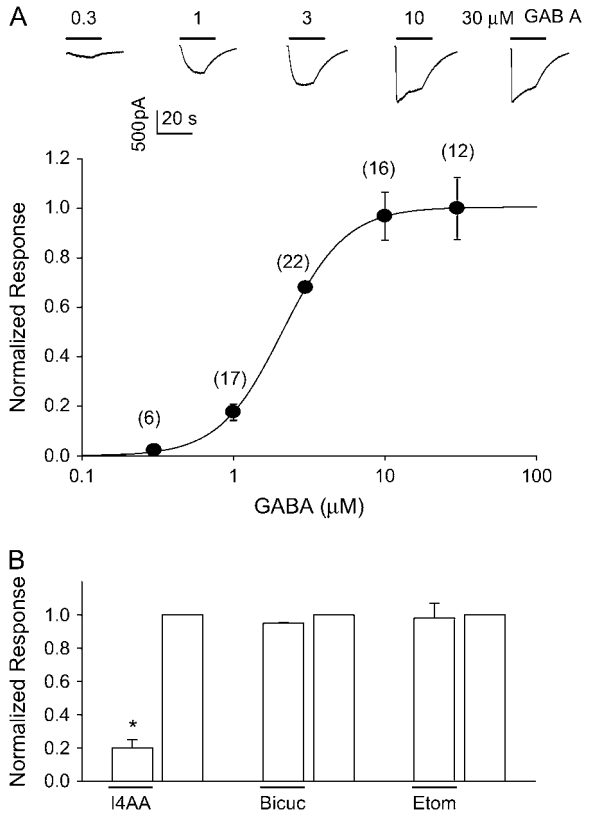


FIGURE 1 GABA concentration-response and pharmacological properties of ρ1 $GABA_C$ receptors expressed in HEK293 cells. (*A, upper*) Representative current traces from a cell voltage-clamped at −60 mV and GABA applied (*line*) by a rapid-perfusion device. Note the current decay observed during the drug application at the higher GABA concentrations. (*A, lower*) A concentration–response relationship derived from the measured peak current magnitude normalized to the response to 3 μM GABA. The continuous curve is a Hill equation with an EC50 = 2.11 μM, $n = 2.08$ fit to the data points. The model fit using the optimized rate constants (see Table 1) gave an EC50 = 2.15 and $n = 2.09$, completely overlapping the empirical data. The number of independent observations is noted within the parentheses. (*B*) Pharmacological response of the GABA-evoked currents to I4AA (100 μM), bicuculline (100 μM), and etomidate (8.2 μM). [GABA] was 100 μM for the I4AA and bicuculline experiments but 3 μM for etomidate because a non-saturating concentration of GABA was desirable to detect possible potentiation of the current by etomidate. $n = 5$–8 cells for each, and * denotes $p < 0.05$ by a two-tailed *t*-test.

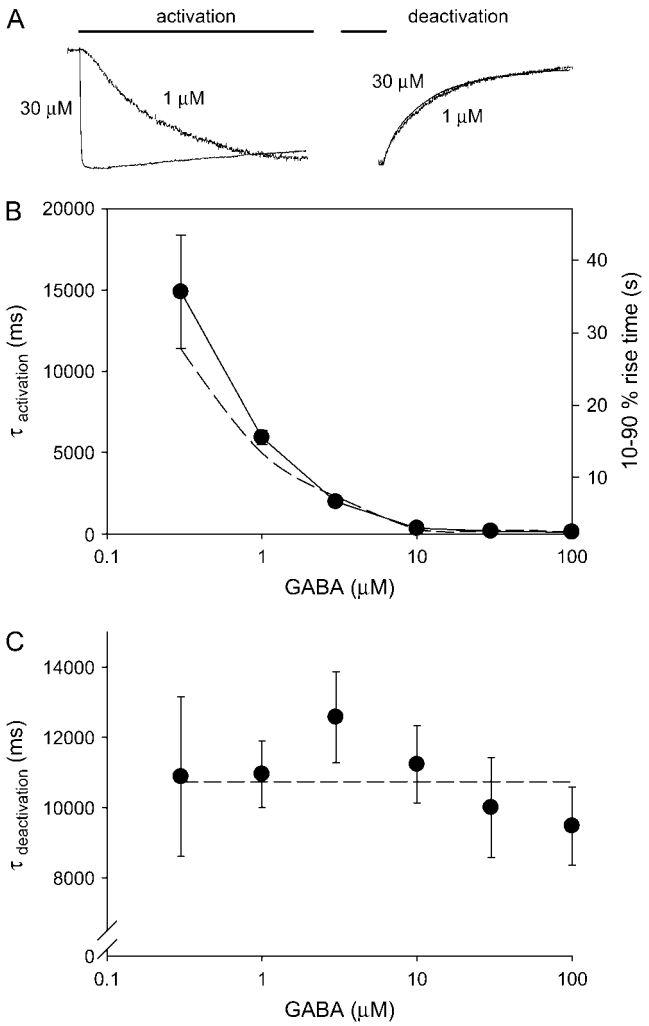


FIGURE 2 Kinetic properties of ρ1 receptors. (*A*) Representative current traces to 1 or 30 μM GABA application showing the activation (*left*) and the deactivation (*right*) phases of the responses. (*B*) The activation phase of the current was approximated by a monoexponential function and the time constant of activation ($\tau_{activation}$) plotted for different GABA concentrations. The limiting activation time constant was 101 ± 6.4 ms ($n = 7$). The same data plotted as a 10–90% rise time (*right axis*) corresponding to the monoexponential time constant axis. (*C*) The same as above except for the current deactivation. For both panels, the dotted lines represent the model prediction using the optimized parameters.

bicuculline, not potentiated by etomidate, but blocked by I4AA (Fig. 1 *B*), confirming the general pharmacological properties expected of the ρ1 receptors.

A careful examination of the rising phase of the current showed complex kinetics with an obvious initial sigmoidal take-off clearly visible for the slowly activating current at the low GABA concentration (Fig. 2 *A*). Therefore, the activation rate was quantified as both a 10–90% rise time and a monoexponential activation time constant ($\tau_{activation}$) (Fig. 2 *B*). However, as the activation rate increased with increasing GABA concentration, the time course of the current was well approximated by a monoexponential function. Kinetic analysis of the current revealed a GABA concentration-dependent acceleration of the activation rate reaching an asymptote of ~10 $s^{-1}$ at 100 μM GABA. The decay of the current on removal of GABA or the current deactivation was mostly monoexponential with a time constant of $\tau_{deactivation}$ and independent of GABA concentration (Fig. 2 *C*).

ρ1 homomeric receptors expressed in the *Xenopus* oocytes showed no desensitization; however, the current magnitude recorded from the HEK cells clearly decreased with time in the presence of constant GABA. This apparent desensitization varied from cell to cell even for the same concentration of GABA (Fig. 3 *A*). In fact, a scatter plot of the monoexponential time constant fit to the apparent desensitization

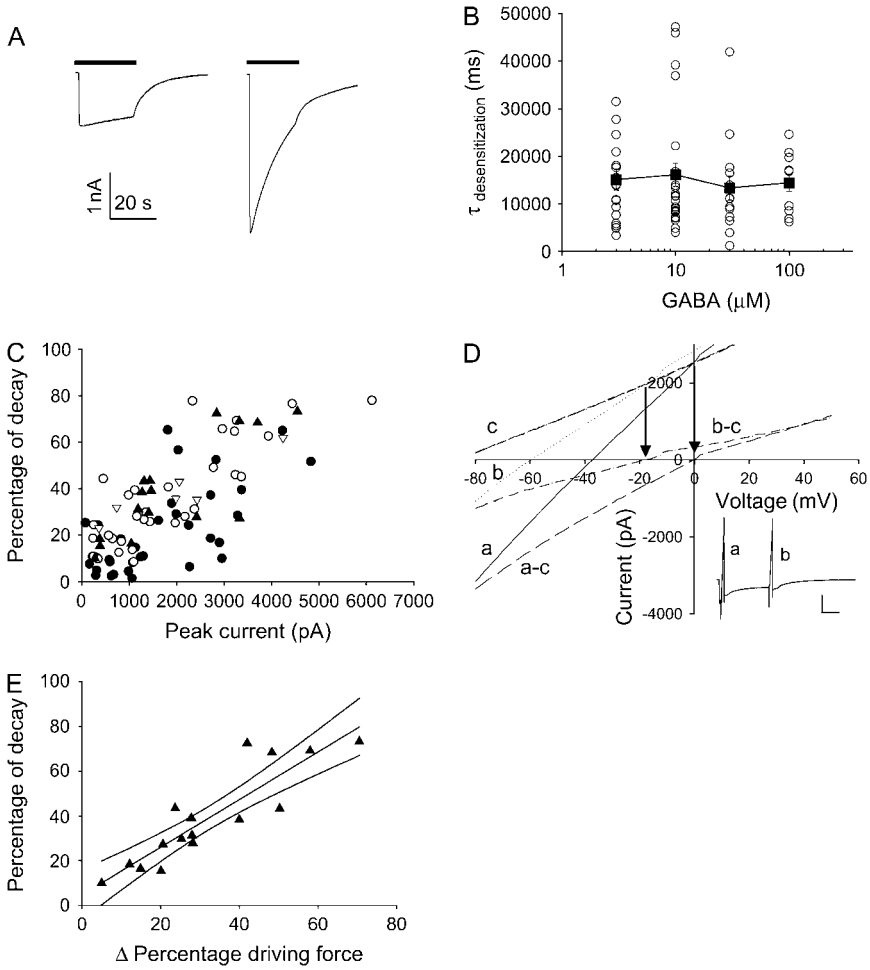


FIGURE 3 Current decay during GABA application correlates with the current magnitude. (*A*) Two examples of current evoked by 30 $\mu$M GABA (*bar*) with extreme differences in the apparent desensitization. Both cells were voltage clamped at −60 mV and had comparable cell capacitance and access resistance. (*B*) A scatter diagram of the apparent desensitization ($\tau_{desensitization}$) for different GABA concentrations. Open circles are individual cells, and the solid square is the mean ± SE. (*C*) A scatter plot of percentage of current decay during GABA application versus peak amplitude for 100 $\mu$M (Δ), 30 $\mu$M (▲), 10 $\mu$M (○), and 3 $\mu$M (●). (*D*) A ramp command voltage (−80 to +50 mV) was issued at different times (*a* near peak and *b* after decline) during a response to 30 $\mu$M GABA application (*inset*), and the resulting *I-V* curve calculated as the difference between the passive *I-V* obtained before GABA application (heavy dashed *c*) and the active *I-V* curves (dot *b* and line *a*), demonstrated a shift of $E_{Cl}$ from 0 mV to −20 mV. For this particular cell, the passive *I-V* curve demonstrated a linear input resistance of ~32 MΩ. Arrows denote the apparent reversal potential defined as the intersection between the passive and active *I-V* curves. (*E*) A scatter plot of 16 cells examined at 30 $\mu$M GABA with the best fitting linear correlation with 95% confidence interval ($r^2 = 0.79$) between the percentage of current decay and percentage change in driving force as determined by the ramp *I-V* experiments.

showed no GABA concentration dependence (Fig. 3 *B*), arguing against a true desensitization or the entry of a GABA-bound channel into a nonconductive state. Further analysis of the data showed that the magnitude of apparent desensitization correlated well with the initial current magnitude (Fig. 3 *C*), suggesting a possible time-dependent decrease in the chloride reversal potential as a possible mechanism for the apparent receptor desensitization. A direct assessment of the chloride reversal potential by issuing a ramp-command voltage at the beginning and the end of the decreasing GABA-evoked current confirmed a shift in the chloride reversal potential (Fig. 3 *D*). Overall, the shift in the driving force accounted for the decrease in the current magnitude well (Fig. 3 *E*). Therefore, the time-dependent decrease in the current magnitude was not caused by receptor desensitization but rather by a decreased driving force from chloride ion depletion within the patch-clamped cell.

To gain a better quantitative understanding of the channel behavior, we sought the optimized rate constants for the five-state kinetic model (Fig. 4 *A*) that best describe the experimental data. A kinetic simulation was implemented in Matlab, and the model parameters optimized based on a global sum squared error measure. The simulated current as a function of time and the steady-state GABA concentration–response relationship are shown in Fig. 4, *B* and *C*, respectively. The concentration-response predicted from the oocyte parameter set is shown for comparison (Fig. 4 *C*, *open squares*). The GABA concentration-independent deactivation time constant was ~11 s, and the limiting monoexponential current activation at high [GABA] was 0.1 s (i.e., $1/(\alpha + \beta)$). Table 1 lists the optimized rate constants and some predicted properties of the present model compared to the kinetic model derived from the same $\rho$1 subunit expressed in the *Xenopus* oocyte (4). All four rate constants governing the channel behavior are different, but the most notable is the significantly faster $K_{off}$ (0.18 $s^{-1}$ for *Xenopus* oocytes and 4.59 $s^{-1}$ for HEK cells). The model quantitatively recapitulated the experimental steady-state concentration-response (Fig. 1, *solid line*), the activation (Fig. 2 *B*, *dashed line*), and deactivation (Fig. 2 *C*, *dashed line*) kinetics well.

Next, the chloride ion shift responsible for the decline in the current magnitude during GABA application was incorporated into the model. Assuming the initial chloride concentration inside the cell $[Cl]_{i,0} = 140$ mM, the

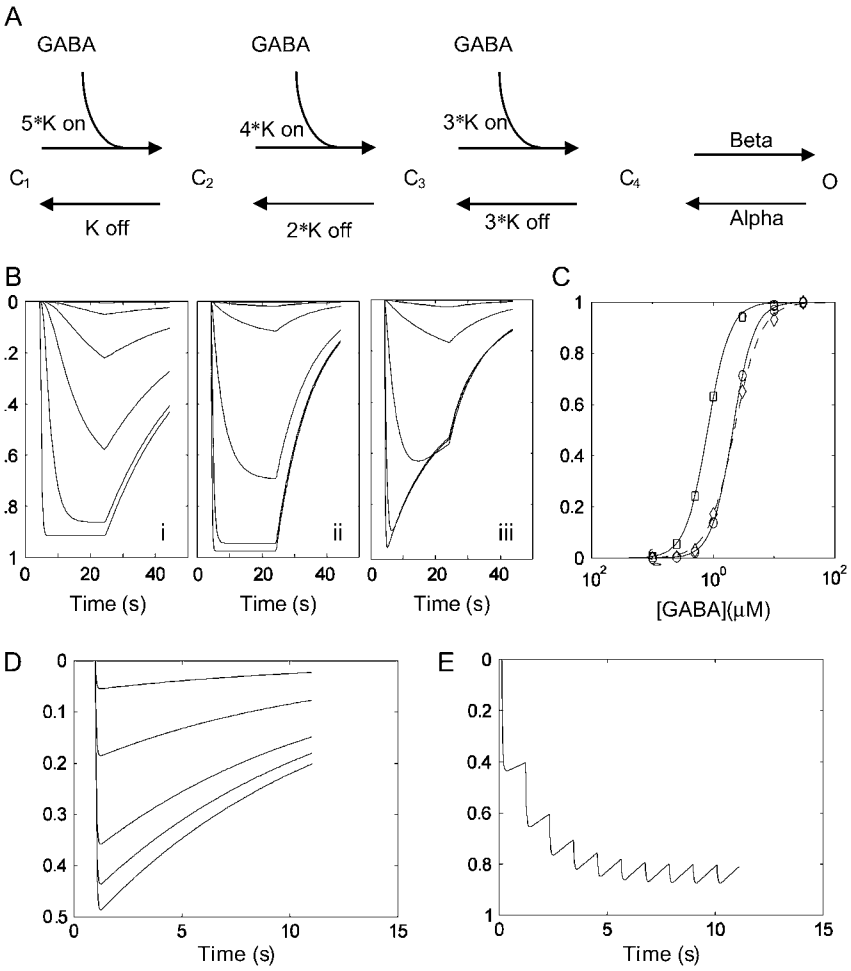


FIGURE 4 A kinetic model of ρ1 $GABA_C$ channels and simulations based on the optimized rate constants. (*A*) A five-state model of ρ1 channel previously used to explain the kinetic behavior of the same subunit expressed in *Xenopus* oocytes (4). The model consists of three identical GABA binding sites and a single transition of the fully bound receptor ($C_4$) to an open state (O). (*B*) A plot of simulated probability of opening versus time for the oocyte parameter set (*i*), optimized HEK cell parameter set (*ii*), and as in *ii* but incorporating an $E_{Cl}$ shift into the model (see Table 1). (*C*) Simulated concentration-response curves based on the peak conductance attained during the GABA application without (*circle*) or with (*diamond*) the $E_{Cl}$ shift. Note the slight underestimation of the peak current magnitude at high [GABA] caused by the loss of driving force and a slight rightward shift of the estimated concentration–response curve (*dashed line*). The oocyte parameter set results in a leftward shifted concentration–response curve (*square*). (*D*) Simulated responses to 1 mM GABA pulses of different durations (1, 2, 5, 10, 20 ms). (*E*) A response to a slow train (1 Hz) of 1 mM GABA pulses. Note the saturation of the conductance because of the slow deactivation kinetics even at this very slow rate of action potential train. The vertical axis represents the probability of channel opening $p(o)$ except for the simulation incorporating the $E_{Cl}$ shift (*Biii*), which represents the normalized macroscopic current $I(t)/N^*\gamma = p(o)^*(V_m - E_{Cl})$, where $N$ = channel number, $\gamma$ = single-channel conductance, $p(o)$ = probability of channel opening, $V_m$ = membrane potential, and $E_{Cl} = Cl^-$ Nernst potential.

discrete time-dependent change in $[Cl]_{i,t+\Delta t}$ as a result of the chloride flux = $I_t$ (coul/s)/$F$ (coul/mol) was determined, and the current at a discrete time $t + \Delta t$ calculated as $I_{t+\Delta t} = K * p_{t+\Delta t} * (V_m - E_{Cl,t+\Delta t})$ where $K$ ($S$) is a constant dependent on the cell size, single-channel conductance empirically determined for each cell, and channel density; $p$ = probability of channel being in the open state; $V_m = -60$ mV, and $E_{Cl,t+\Delta t} = 58 \log([Cl]_{i,t+\Delta t} / [Cl]_o)$ mV. The resulting current magnitude showed a time-dependent decline despite the constant probability of channel being open during GABA application (Fig. 4 *B*, *iii*). Because the time-dependent $E_{Cl}$ shift and a decrease in the driving force resulted in an underestimation of the peak current, a slight rightward shift of the EC50, and an underestimation of the Hill slope (Fig. 4 *C*, *dashed line*) were observed.

The potential role of receptors with these properties in a traditional fast synapse was simulated by examining the response of channels with the above kinetic properties to a brief pulse of 1 mM GABA. A 1-ms duration pulse typical of a fast presynaptic transmitter release time course yielded only a peak $p$(open) of 0.04 and approached 0.5 for a very long pulse of 20-ms duration (Fig. 4 *D*). As expected from channels with a slow deactivation time constant, the $p$(open) to a 1-Hz train of 10-ms pulses saturates within five pulses, indicating that a synapse populated with these receptors will serve as a poor transducer of dynamic information (Fig. 4 *E*).

The ρ1 subunit may form a heterologous receptor in combination with the $GABA_A$ receptor γ2 subunit (10). Such coassembly of the ρ1 subunit into a nonhomologous receptor could create channels with novel properties. Because HEK293 cells do not express the $GABA_A$ receptor γ2 subunit (11; unpublished observations), we examined the kinetic properties of the bicuculline-resistant current recorded from cultured hippocampal neurons transduced with the ρ1-subunit-expressing adenovirus (7). Coapplication of GABA (100 μM) and the $GABA_A$ receptor blocker bicuculline (100 μM) revealed a smaller bicuculline-resistant component in virally transduced neurons (Fig. 5 *A*). This bicuculline-resistant current was previously demonstrated to be I4AA sensitive and represents current flowing through the expressed ρ1 receptor (7). The kinetic properties of current activation and deactivation of this bicuculline-resistant current were indistinguishable from the homologous ρ1 receptors expressed in HEK293 cells (Fig. 5 *B*), suggesting that no

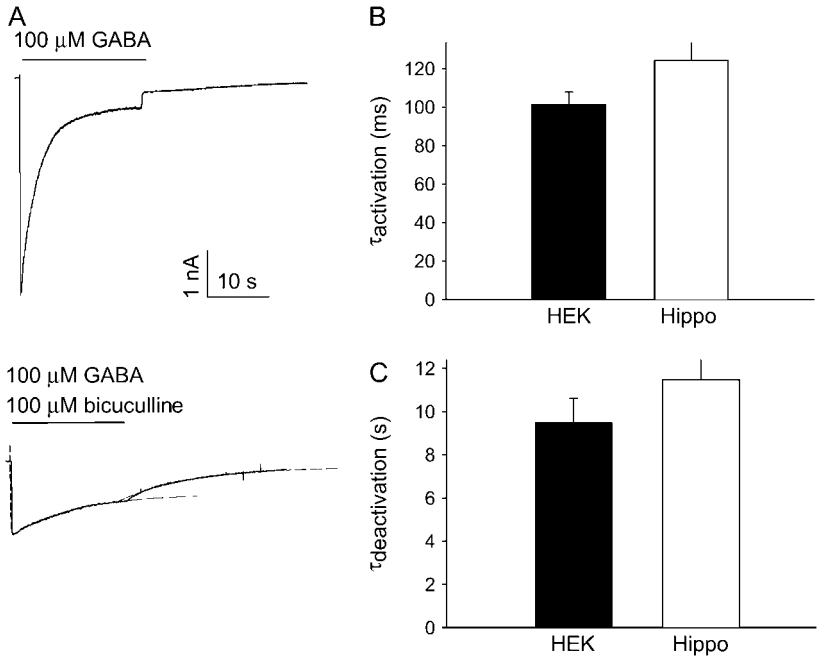


FIGURE 5 Current decay during GABA application is observed in hippocampal neurons expressing the $\rho$1 subunit. (*A*) Current traces of GABA (100 $\mu$M)–evoked responses in a hippocampal neuron transduced with an adenovirus expressing the $\rho$1-subunit without (*top*) or with (*bottom*) coapplication of 100 $\mu$M bicuculline. The dashed lines are the best-fitting monoexponential function fit to the activation and the deactivation phases of the bicuculline-resistant current. See Cheng et al. (7) for further details on the $\rho$1 subunit-expressing adenovirus. (*B*) A bar diagram summary of the approximate monoexponential time constant of activation (*top*) and deactivation (*bottom*) for HEK293 cells ($n = 12$) and hippocampal neurons ($n = 37$); $p = 0.178$ for activation and $p = 0.192$ for deactivation time constants based on a two-tailed *t*-test; thus, the difference in mean was not statistically significant for either measure.

channels with novel kinetic properties emerged even in the presence of numerous other endogenous $GABA_A$ receptor subunits present in the hippocampal neurons.

## DISCUSSION

Analysis of GABA-evoked currents in HEK293 cells transfected with the human $\rho$1 subunit revealed channels less sensitive to GABA with a faster deactivation kinetic compared to the same subunit expressed in the *Xenopus* oocytes. Parameter estimation demonstrated that the experimentally observed properties of the current could be accounted for by the same five-state kinetic model employed to describe the currents obtained in *Xenopus* oocytes but with a much larger dissociation rate constant $K_{off}$. Our data quantitatively differ from those reported by Filippova et al. (5), where EC50 = 0.75 $\mu$M and Hill = 3.14 but agree in the observation that the current deactivation time constant was around 11 s. The reason for this discrepancy is unclear, but parameter estimation based on their target data (assuming a limiting activation rate $\alpha + \beta = 10\ s^{-1}$ not reported in their study) yielded $\alpha = 0.13\ s^{-1}$, $\beta = 9.89\ s^{-1}$, $K_{on} = 1.49\ \mu M^{-1}s^{-1}$, $K_{off} = 8.31\ s^{-1}$, which are qualitatively not different from our stated results. The conclusion remains that the same $\rho$1 receptor expressed in the oocytes or HEK cells demonstrates different kinetic behavior.

Ion channel proteins do not exist in isolation but rather interact with associated proteins, and the presence or absence of the potential partner proteins most likely accounts for the expression of system-dependent differences in the channel function. Two-hybrid screening has identified the cytoskeletal protein MAP-1B (12), a splice variant of the glycine transporter GLYT-1 (13), and a protein kinase $\zeta$-interacting protein ZIP3 (14) as likely protein partners interacting with the $\rho$-subunits. The interaction between the $\rho$-subunits and MAP-1B increases the sensitivity of the receptor, doubling the current magnitude elicited by low concentrations of GABA (15). Further receptor diversity is introduced by the likely interaction among the three $\rho$-subunits (16,17) all coexisting within a single hippocampal pyramidal or granule cell (18). Direct coimmunoprecipitation experiments support the notion that the $\rho$ subunit protein biochemically interacts with the $GABA_A$ receptor $\alpha_1$ and $\gamma_2$ subunits (19). The functional consequence of this interaction may be acceleration of the deactivation kinetics (10) and creation of receptors exhibiting mixed $GABA_A$ and $GABA_C$ pharmacology (20,21).

HEK293 cells do not express endogenous $\rho$ or $GABA_A$ subunits, although one report suggested a possible expression of an endogenous $GABA_A$ $\beta$-like subunit in these cells (11). It is unknown whether any of the other identified protein partners are expressed in the HEK293 cells, but the $\rho$1 subunit interacting with a $GABA_A$ subunit as the reason for the observed channel behavior is unlikely. The similarity of the current activation and deactivation kinetics observed in HEK cells and when the $\rho$1 subunit was expressed in the hippocampal neurons with abundant potential $GABA_A$ subunit partners present supports this conclusion. The functionally significant putative $\rho$1 protein partner is likely to exist in the HEK cells and hippocampal neurons.

Given the kinetic behavior of $\rho$1 receptors expressed in a mammalian cell, what are the implications for a possible synaptic response mediated by these receptors? The simulated response to a brief but high-concentration GABA application to these receptors most likely to occur at a fast

synapse showed the activation rate to be too slow to mount a significant postsynaptic response. A 1 mM GABA pulse approaching 10 ms was necessary for eliciting any appreciable current. Furthermore, the slow deactivation rate limited the ability of synapses mediated by the $\rho$1 receptors to dynamically respond to even a very slow train of action potentials without saturating the response. Therefore, $\rho$1 receptors with the observed kinetics are unlikely to mediate a fast synaptic response but more likely to play a role in setting the background conductance level of a neuron more akin to the tonic inhibitory receptors discovered in the hippocampus (22). A $GABA_C$ receptor-mediated synaptic response in retinal bipolar cells evoked by electrical stimulation of the inner plexiform layer of the retina exhibited a time course well described by a biexponential decay with time constants of 125 and 1351 ms (23), thus exhibiting much faster deactivation not recapitulated by the $\rho$1 subunits expressed in HEK293 cells or the hippocampal neurons. The $\rho$1-protein component of the $GABA_C$ receptor subserving a synaptic function in the retina must be interacting with protein partners not present in the HEK293 cells or the hippocampal neurons to accelerate the deactivation kinetics by almost 10-fold.

Direct measurement of ramp *I-V* curves during GABA application with a proper subtraction of the passive conductance demonstrated that an $E_{Cl}$ shift was responsible for the apparent desensitization of the $\rho$1 receptors in HEK293 cells. Our technical limitation with uncompensated series resistance underreports the true current magnitude, particularly at the beginning of GABA application when the current is large. Despite this limitation, our analysis confirmed that a reduction in the driving force mostly accounted for the apparent desensitization. An $E_{Cl}$ shift contributing to an apparent desensitizing GABA-evoked current in patch-clamped hippocampal cells was first reported by Huguenard and Alger (24). Filippova et al. (5) observed a current decline mediated by $\rho$1 receptors expressed in HEK293 cells when the current was greater than 1 nA, similar to the apparent desensitizing responses seen in our experiments. However, our channel simulation taking into account the $E_{Cl}$ shift demonstrated that the slow time course decrease in the current had little effect on the concentration-response or the time course of activation and deactivation, suggesting that the quantitative model parameters based on our experimental data remain valid. Synaptically activated currents are surely much smaller than the levels of currents observed in the experimental systems with overexpressed receptors. In contrast, the cellular volume of the postsynaptic dendritic spine is orders of magnitude smaller than the whole-cell patch-clamped cells. Therefore, an $E_{Cl}$ shift caused by chloride ion accumulation could contribute to a decline in the long-term efficacy of an inhibitory synapse.

We presented a quantitative set of rate constants describing the behavior of the $\rho$1 homomeric receptors expressed in HEK293 cells significantly different from the values obtained from similar experiments in *Xenopus* oocytes. We suggest that the parameter set for a five-state model of the $\rho$1 homomeric receptor described in our work may better describe the behavior of these channels in mammals.

This work was supported by grants RO1 GM52325 and NS45718 and funds from the Department of Anesthesiology at Columbia University College of Physicians & Surgeons.

## REFERENCES

1. Shimada, S., G. Cutting, and G. R. Uhl. 1992. $\gamma$-Aminobutyric acid A or C receptor? $\gamma$-Aminobutyric acid $\rho$1 receptor RNA induces bicuculline-, barbiturate-, and benzodiazepine-insensitive $\gamma$-aminobutyric acid responses in *Xenopus* oocytes. *Mol. Pharmacol.* 41:683–687.
2. Amin, J., and D. S. Weiss. 1994. Homomeric $\rho$1 GABA channels: Activation properties and domains. *Receptors Channels.* 2:227–236.
3. Amin, J., and D. S. Weiss. 1996. Insights into the activation mechanism of $\gamma$1 GABA receptors obtained by coexpression of wild type and activation-impaired subunits. *Proc. R. Soc. Lond. B Biol. Sci.* 263: 273–282.
4. Chang, Y., and D. S. Weiss. 1999. Channel opening locks agonist onto the $GABA_C$ receptor. *Nat. Neurosci.* 2:219–225.
5. Filippova, N., R. Dudley, and D. S. Weiss. 1999. Evidence for phosphorylation-dependent internalization of recombinant human $\rho$1 $GABA_C$ receptors. *J. Physiol.* 518:385–399.
6. Filippova, N., A. Sedelnikova, W. J. Tyler, T. L. Whitworth, H. Fortinberry, and D. S. Weiss. 2001. Recombinant $GABA_C$ receptors expressed in rat hippocampal neurons after infection with an adenovirus containing the human $\rho$1 subunit. *J. Physiol.* 535:145–153.
7. Cheng, Q., J. C. Kulli, and J. Yang. 2001. Suppression of neuronal hyperexcitability and associated neuronal death by adenoviral expression of $GABA_C$ receptors. *J. Neurosci.* 21:3419–3428.
8. Wotring, V. E., Y. Chang, and D. S. Weiss. 1999. Permeability and single channel conductance of human homomeric $\rho$1 $GABA_C$ receptors. *J. Physiol.* 521:327–336.
9. Colquhourn, D., and A. G. Hawkes. 1995. A Q-matrix cookbook. *In* Single Channel Recording, 2nd Ed. B. Sakmann and E. Neher, editors. Plenum Press, New York. 589–633.
10. Qian, H., and H. Ripps. 1999. Response kinetics and pharmacological properties of heteromeric receptors formed by coassembly of GABA rho- and gamma 2-subunits. *Proc. R. Soc. Lond. B Biol. Sci.* 266:2419–2425.
11. Ueno, S., C. Zorumski, J. Bracamontes, and J. H. Steinbach. 1996. Endogenous subunits can cause ambiguities in the pharmacology of exogenous $\gamma$-aminobutyric acid A receptors expressed in human embryonic kidney 293 cells. *Mol. Pharm.* 50:931–938.
12. Hanley, J. G., P. Koulen, F. Bedford, P. R. Gordon-Weks, and S. J. Moss. 1999. The protein MAP-1B links GABAC receptors to the cytoskeleton at retinal synapses. *Nature.* 397:66–69.
13. Hanley, J. G., E. M. C. Jones, and S. J. Moss. 2000. GABA receptor $\rho$1 subunit interacts with a novel splice variant of the glycine transporter, GLYT-1. *J. Biol. Chem.* 275:840–846.
14. Croci, C., J. H. Brandstatter, and R. Enz. 2003. ZIP3, a new splice variant of the PKC-$\varepsilon$-interacting protein family, binds to $GABA_C$ receptors, PKC-$\varepsilon$, and K$v\beta$2. *J. Biol. Chem.* 278:6128–6135.
15. Billups, D., J. G. Hanley, M. Orme, D. Attwell, and S. J. Moss. 2000. $GABA_C$ receptor sensitivity is modulated by interaction with MAP1B. *J. Neurosci.* 20:8643–8650.
16. Ogurusu, T., K. Yanagi, M. Watanabe, M. Fukuya, and R. Shingai. 1999. Localization of GABA receptor rho2 and rho3 subunits in rat brain and functional expression of homoligomeric rho3 receptors and heteroligomeric rho2-rho3 receptors. *Receptors Channels.* 6:463–475.
17. Enz, R., and G. R. Cutting. 1999. $GABA_C$ receptor rho subnits are heterogeneously expressed in the human CNS and form homo- and heterooligomers with distinct physical properties. *Eur. J. Neurosci.* 11:41–50.

18. Liu, B., N. Hattori, B. Jiang, Y. Nakayama, N. Y. Zhang, B. Wu, K. Kitagawa, M. Taketo, H. Matsuda, and C. Inagaki. 2004. Single cell RT-PCR demonstrates differential expression of $GABA_C$ receptor rho subunits in rat hippocampal pyramidal and granule cells. *Brain Res. Mol. Brain Res.* 123:1–6.

19. Milligan, C. J., N. J. Buckley, M. Garrett, J. Deuchars, and S. A. Deuchars. 2004. Evidence for inhibition mediated by coassembly of $GABA_A$ and $GABA_C$ receptor subunits in native central neurons. *J. Neurosci.* 24:7241–7250.

20. Schlicker, K., M. Boller, and M. Schmidt. 2004. $GABA_C$ receptor mediated inhibition in acutely isolated neurons of the rat dorsal lateral geniculate nucleus. *Brain Res Bull.* 63:91–97.

21. Hartmann, K., F. Stief, A. Draguhn, and C. Frahm. 2004. Ionotropic GABA receptors with mixed pharmacological properties of $GABA_A$ and $GABA_C$ receptors. *Eur. J. Pharmacol.* 497:139–146.

22. Mody, I., and R. A. Pearce. 2004. Diversity of inhibitory neurotransmission through $GABA_A$ receptors. *Trends Neurosci.* 27:569–575.

23. Lukasiewicz, P. D., and C. R. Shields. 1998. Different combinations of $GABA_A$ and $GABA_C$ receptors confer distinct temporal properties to retinal synaptic responses. *J. Neurophysiol.* 79:3157–3167.

24. Huguenard, J. R., and B. E. Alger. 1986. Whole-cell voltage-clamp study of the fading of GABA-activated currents in acutely dissociated hippocampal neurons. *J. Neurophysiol.* 56:1–18.